

RESEARCH ARTICLE

Efficient removal of harmful algae from eutrophic natural water by $\text{Mg}(\text{OH})_2$ coated nanoscale zero-valent iron

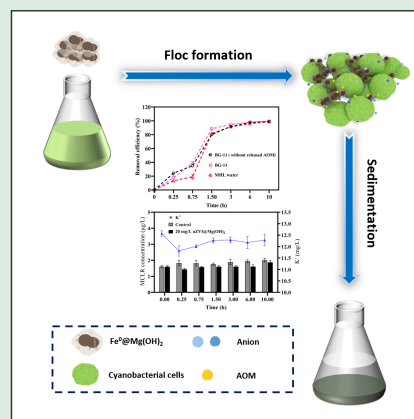
Zhanyu Ge¹, Xuegang Chen², Jiajia Fan ¹

1. School of Life and Environmental Sciences, Hangzhou Normal University, Hangzhou 311121, China

2. Ocean College, Zhejiang University, Hangzhou 310058, China


HIGHLIGHTS

- $\text{Fe}^0@\text{Mg}(\text{OH})_2$ effectively removed cyanobacteria with high cell densities.
- The impacts of various factors on the efficiency of $\text{Fe}^0@\text{Mg}(\text{OH})_2$ were determined.
- The *in situ* formed Fe(III) assisted the removal of cyanobacterial cells.
- The release of MCs and AOM was negligible during $\text{Fe}^0@\text{Mg}(\text{OH})_2$ treatment.



ABSTRACT: Iron-based nanoparticles have recently been developed to mitigate cyanobacterial blooms. In this study, a method utilizing $\text{Mg}(\text{OH})_2$ coated nanoscale zero-valent iron ($\text{Fe}^0@\text{Mg}(\text{OH})_2$) was applied to treat cyanobacteria (*Microcystis aeruginosa*) in natural water. The influence of initial cell densities, $\text{Fe}^0@\text{Mg}(\text{OH})_2$ dosages, and water matrix on the removal efficiency of *M. aeruginosa* was systematically explored. Higher removal efficiencies of *M. aeruginosa* were achieved with increased initial cell densities, probably because larger amounts of cells and associated dissolved algal organic matters (AOM) promoted the formation and sedimentation of cell- $\text{Fe}^0@\text{Mg}(\text{OH})_2$ -AOM complexes. About 98.7% of *M. aeruginosa* cells (initial cell density = 1.0×10^6 cells/mL) were removed after treatment with 20 mg/L $\text{Fe}^0@\text{Mg}(\text{OH})_2$ for 10 h, despite anions (e.g., SO_4^{2-}) in natural water reduced the removal efficiency in the first 1.5 h. Most of the *M. aeruginosa* cells maintained intact during $\text{Fe}^0@\text{Mg}(\text{OH})_2$ treatment, as confirmed by the observation of their ultrastructure and the measurement of K^+ and Chlorophyll a concentrations. As a result, the release of microcystins and AOM was negligible during the treatment. This study demonstrates that $\text{Fe}^0@\text{Mg}(\text{OH})_2$ is a promising approach for effective treatment of waters with high concentrations of cyanobacteria, without posing increased ecological risks.

KEYWORDS: Algal removal, Influencing factors, $\text{Fe}^0@\text{Mg}(\text{OH})_2$, Microcystin

 Corresponding author. E-mail: fanjiajia@hznu.edu.cn

Article history: Received 21 November 2024, Revised 7 January 2025, Accepted 23 January 2025, Available online 6 March 2025

© Higher Education Press 2025

Special Issue—Microbiological Contaminants in Water Environment: Occurrence and Control (Responsible Editors: Xin Yu, Hong Chen & Yunho Lee)

1 Introduction

Owing to global climate change and dramatic increasing bioavailable nutrients in surface waters, blooms of cyanobacteria (blue-green algae) have occurred frequently worldwide in recent decades (Paerl and Scott, 2010; Gobler, 2020). As a dominant species in these blooms, *Microcystis aeruginosa* can produce various harmful metabolites, including taste and odor compounds, and microcystins (MCs, a type of hepatotoxic cyanotoxins detrimental to animals and humans) (Codd et al., 2005; Zhang et al., 2013). In addition, the excessive growth of *M. aeruginosa* cells leads to the release of algal organic matters (AOM), impairing water quality (Jia et al., 2018). AOM may also negatively affect water treatment processes by reducing coagulation efficiency, causing serious membrane fouling, and acting as precursors of disinfection by-products (Fang et al., 2010; Xie et al., 2013; Li et al., 2014; Zhang et al., 2016).

Conventional water treatments including coagulation, sedimentation, and filtration are ineffective in cyanobacterial removal. Moreover, a combination of those methods is relatively complex and costly (Ma et al., 2007; Rajasekhar et al., 2012; Zamyadi et al., 2012). Addition of oxidants (e.g., chlorine) can improve the subsequent removal of cyanobacteria, but it may also rupture cyanobacterial cells, leading to the release of intracellular toxins and AOM (Huo et al., 2015; Naceradska et al., 2017). Therefore, alternative techniques are required to efficiently remove cyanobacterial cells and minimize the release of harmful metabolites into surrounding waters.

Nanoscale zero-valent iron (Fe^0) has been emerged as a technique for mitigating cyanobacteria problems in recent years. However, its effectiveness in removing and inhibiting cyanobacteria is limited, probably because of the agglomeration and rapid-oxidation of Fe^0 in aqueous solutions (Marsalek et al., 2012; Lei et al., 2016; Eljamal et al., 2018; Nguyen et al., 2018; Chen et al., 2021). Recently, $\text{Mg}(\text{OH})_2$ coated Fe^0 nanoparticles ($\text{Fe}^0@ \text{Mg}(\text{OH})_2$), recognized as an efficient material, have attracted extensive attention. The $\text{Mg}(\text{OH})_2$ shell can protect Fe^0 from rapid corrosion and reduce the magnetic attraction between Fe^0 particles (Hu et al., 2018; Chen et al., 2021). A study by Fan et al. (2018a) has shown that the effectiveness of *M. aeruginosa* removal via $\text{Fe}^0@ \text{Mg}(\text{OH})_2$ greatly increased to 99.9% after 3 h, in contrast to 39.5% by bare Fe^0 . Although *M. aeruginosa* cells remained intact during $\text{Fe}^0@ \text{Mg}(\text{OH})_2$ treatment, as observed by scanning electron microscopy (SEM), the quantitative impact on the release of MCs and AOM

remains unknown, necessitating further investigation.

To date, reported *M. aeruginosa* treatment by $\text{Fe}^0@ \text{Mg}(\text{OH})_2$ was conducted in the BG-11 medium, with a cell density of 2.5×10^6 cells/mL (Fan et al., 2018a). However, the effectiveness of cyanobacteria treatment by various technologies are affected by multi-factors such as background water matrix, chemical dosages, and initial cell densities (Zamyadi et al., 2012; Zhang et al., 2015; Jian et al., 2019). For examples, high concentrations of dissolved organic carbon and various ions in source waters can inhibit K_2FeO_4 oxidation in *M. aeruginosa* inactivation (Fan et al., 2018b). Lin et al. (2009) demonstrated that the rate constants of *M. aeruginosa* cell rupture by chlorination decreased from 180 to 110 mol/(L·s), when the initial cell density increased from 1.3×10^5 to 4.4×10^5 cells/mL. The influence of cell density is expected to be larger since *M. aeruginosa* cell densities can vary from 10^4 to 10^9 cells/mL in natural blooms (Ger et al., 2014; Ma et al., 2015). Therefore, it is important to evaluate those factors on the effectiveness of $\text{Fe}^0@ \text{Mg}(\text{OH})_2$ in treating *M. aeruginosa*, for ensuring its application under practical conditions.

Consequently, the aims of this study were to (1) assess the influence of various factors (initial cell densities, $\text{Fe}^0@ \text{Mg}(\text{OH})_2$ dosages, and water matrices) on the removal efficiency of *M. aeruginosa* by $\text{Fe}^0@ \text{Mg}(\text{OH})_2$ and understand the underlying mechanisms; (2) investigate the viability of *M. aeruginosa* cells in natural water by $\text{Fe}^0@ \text{Mg}(\text{OH})_2$ treatment; and (3) explore the concomitant release of MCs and AOM during the $\text{Fe}^0@ \text{Mg}(\text{OH})_2$ treatments.

2 Materials and methods

2.1 Water source

Raw water was collected from the Ming Hui Lake (MHL) (where cyanobacterial blooms occur frequently) located in Zhoushan, China. The sampled water was filtered through 0.45 μm and then 0.22 μm cellulose acetate filters (Xingya, China) to remove impurities and microorganisms. The filtered source water was then stored at 4 °C for the subsequent experiments, its qualities were presented in Table S1.

2.2 Cultures of *M. aeruginosa*

M. aeruginosa (strain FACHB-905, from the Institute of Hydrobiology, Chinese Academy of Sciences, China) was chosen as the target cyanobacterium. *M. aeruginosa* was cultured in sterilized basal glucose

(BG-11) medium and routinely sub-cultured (Stanier et al., 1971). The strain was incubated under cool fluorescent light flux ($25 \mu\text{mol}/(\text{m}^2\cdot\text{s})$), light-dark cycle = 12 h:12 h), at a constant temperature of $25 \pm 1 \text{ }^\circ\text{C}$ to achieve healthy *M. aeruginosa* cultures.

2.3 Synthesis of $\text{Fe}^0\text{@Mg}(\text{OH})_2$

The $\text{Fe}^0\text{@Mg}(\text{OH})_2$ particles were chemically prepared based on a rate-controlled precipitation method as per Hu et al. (2019). In general, 70 mg Fe^0 was suspended into ethanol by ultrasonically dispersing under N_2 atmosphere at $25 \pm 2 \text{ }^\circ\text{C}$ to avoid oxidation. Subsequently, a certain amount of MgCl_2 /ethanol solution was added to the suspension to ensure the ration of Mg/Fe (wt%) was 1:2. The concentrations and dropping speed of the NaOH/ethanol solutions were controlled to achieve complete reaction. After aged for 1 h under ultrasonic conditions, the $\text{Fe}^0\text{@Mg}(\text{OH})_2$ particles were subsequently washed using methanol and ethanol for three times in turns and dried with N_2 gas.

2.4 *M. aeruginosa* exposure to $\text{Fe}^0\text{@Mg}(\text{OH})_2$

All experiments were performed at a room temperature of $20 \pm 2 \text{ }^\circ\text{C}$. $\text{Fe}^0\text{@Mg}(\text{OH})_2$ was dispersed with deoxygenated deionized water under ultrasonic conditions to prepare nano-particle suspension. Then 5 mL of the suspension contained with certain amount of $\text{Fe}^0\text{@Mg}(\text{OH})_2$ particles was mixed with 95 mL of *M. aeruginosa* culture in 100 mL conical flasks. Air-breathing membranes were used to seal the bottles ensuring gas exchange while preventing cross-contamination. Subsequently, various tests were applied to explore the efficiency of $\text{Fe}^0\text{@Mg}(\text{OH})_2$ on *M. aeruginosa* cell removal, with all tests conducted in triplicates.

2.4.1 Factors on the removal efficiency of *M. aeruginosa* by $\text{Fe}^0\text{@Mg}(\text{OH})_2$

To investigate the removal effects of $\text{Fe}^0\text{@Mg}(\text{OH})_2$ on *M. aeruginosa* samples across varying cell densities, initial cell densities ranging from 1.0×10^5 to 8.0×10^6 cells/mL were prepared by dilution with BG-11 medium. A consistent $\text{Fe}^0\text{@Mg}(\text{OH})_2$ (Fe) concentration of 50 mg/L was employed. Moreover, to explore the impacts of different $\text{Fe}^0\text{@Mg}(\text{OH})_2$ concentrations on *M. aeruginosa* removal, specific volumes of $\text{Fe}^0\text{@Mg}(\text{OH})_2$ suspension were added into *M. aeruginosa* samples (cell density = 1.0×10^6 cells/mL) to achieve the final Fe concentration from 10 to 80 mg/L. In addition, to explore the influences of

water matrix on the removal efficiency of *M. aeruginosa* cells by $\text{Fe}^0\text{@Mg}(\text{OH})_2$, experiments were conducted using BG-11 medium (with and without the released AOM) and MHL water for comparison. The initial cell density of *M. aeruginosa* was set at 1.0×10^6 cells/mL, with $\text{Fe}^0\text{@Mg}(\text{OH})_2$ (Fe) concentration of 20 mg/L. The cell removal efficiency (R) was calculated as followed Eq. (1):

$$R = \frac{N_c - N_t}{N_c} \times 100\%, \quad (1)$$

where N_c and N_t represent the *M. aeruginosa* cell density in the control and $\text{Fe}^0\text{@Mg}(\text{OH})_2$ treated sample at a specific sampling time of t , respectively.

2.4.2 The impacts of $\text{Fe}^0\text{@Mg}(\text{OH})_2$ on characteristics of *M. aeruginosa* cells

According to the results from 2.4.1, *M. aeruginosa* cultures with an initial cell density of 1.0×10^6 cells/mL (diluted with MHL water) were chosen for the experiments involving $\text{Fe}^0\text{@Mg}(\text{OH})_2$ treatment at a Fe concentration of 20 mg/L. Prior to the test, the pH value of *M. aeruginosa* samples was controlled as 8.0 ± 0.1 with 0.1 mol/L NaOH or 0.1 mol/L HCl. Then, *M. aeruginosa* samples collected at pre-determined time intervals were prepared for further analysis. The evaluation of *M. aeruginosa* cell viability was conducted through the detection of Chlorophyll a (Chl-a), Fv/Fm indicating the maximum effective quantum yield of PSII, and potassium ion (K^+) levels. Transmission electron microscopy (TEM, JEM-1230, JEOL, Japan) was utilized to characterize the ultrastructure of *M. aeruginosa* cells. The concentrations of extracellular microcystin-LR (MC-LR) and amounts of the released AOM were measured to assess the subsequent impacts on water quality. X-ray photoelectron spectroscopy (XPS, K-Alpha, Thermo Scientific, USA) and X-ray diffraction (XRD, Ultima IV, Rigaku, Japan) were conducted to investigate the mechanisms of *M. aeruginosa* removal by $\text{Fe}^0\text{@Mg}(\text{OH})_2$.

2.5 Analytical methods

2.5.1 Cell counts

M. aeruginosa samples were collected from 0 to 10 h from the suspensions, and immediately treated with Lugol's iodine. Subsequently, the cell densities were enumerated with a microscopy (ECLIPSE E100, Nikon, Japan) at 100 \times magnification using a Sedgwick Rafter chamber (Graticules Ltd, UK) (Fan et al., 2013).

2.5.2 Characterization of flocs during exposure process

XRD was used to characterize crystal structure of $\text{Fe}^0\text{@Mg}(\text{OH})_2$ after exposure to SO_4^{2-} solutions ($\text{Fe}:\text{SO}_4^{2-} = 1:3$, wt%). The XRD data were performed in an angular range $2\theta = 10\text{--}80^\circ$ with a step length of $0.02^\circ/\text{min}$ and a scanning speed of $5^\circ/\text{min}$. The diffractograms were then compared to International Centre for Diffraction Data (ICDD) cards: brucite 83-0114, Fe^0 87-0721, goethite 81-0462, hematite 85-0987. To analyze the changes in surface composition, the crystals of flocs were characterized by XPS before and after the reaction.

2.5.3 Cell viability

The concentration of Chl-a was estimated according to a previous study [Gao and Tam \(2011\)](#). In brief, Chl-a was extracted from 10 mL *M. aeruginosa* sample with 95% ethanol for 10 min at 60°C . The extraction supernatant was measured subsequently at the wavelength of 665 and 652 nm, and then the amount of Chl-a was calculated based on these readings. The Fv/Fm values of *M. aeruginosa* were quantified after dark-adaptation for 15 min, using a Phyto-Pulse-Amplitude modulated fluorometer (Phyto-PAM, Walz, Germany) ([Wu et al., 2007](#)).

To determine the integrity of *M. aeruginosa* cells during $\text{Fe}^0\text{@Mg}(\text{OH})_2$ treatment, the levels of K^+ and released AOM after treatments were assessed. *M. aeruginosa* sample with a volume exceeding 20 mL (collected at 0.25, 0.75, 1.5, 3, 6, and 10 h, respectively) was successively filtrated through 0.45 and $0.22\ \mu\text{m}$ glass-fiber filters (GF/F, Xingya, China), and then divided into two sub-samples. One filtrate (10 mL) was acidified with concentrated HNO_3 for immediate K^+ detection using an atomic absorption spectrophotometer (200 Series, Agilent Technologies, USA). Another 10 mL filtrated sample was used to analyze the fluorescence excitation-emission matrix (EEM) spectra of the released AOM, with a fluorescence spectrophotometer (RF-6000, Shimadzu, China). Data analysis was referred to a method recorded by [Tang et al. \(2018\)](#). The EEM spectra were collected by scanning the emission wavelength (Em) of 250–550 nm at 2 nm increments, and excitation wavelength (Ex) of 200–450 nm at 5 nm increments.

2.5.4 Quantification of MC-LR

Due to the strong aggregation and binding between the *M. aeruginosa* cells and $\text{Fe}^0\text{@Mg}(\text{OH})_2$ particles, as reported by [Fan et al. \(2018a\)](#), it appears to be

challenging to separate the cells from the sediment. Consequently, only extracellular MC-LR was determined in this study. Following exposure to $\text{Fe}^0\text{@Mg}(\text{OH})_2$ for 0.25, 0.75, 1.5, 3, 6, and 10 h, 100 mL *M. aeruginosa* suspension was collected and subsequently filtered through 0.45 and $0.22\ \mu\text{m}$ membrane filters to analyze the amount of extracellular toxin. The filtrates were then concentrated using C18 solid-phase (Waters, USA) extraction ([Nicholson et al., 1994](#)). The concentrations of extracellular MCs were quantified using a high-performance liquid chromatography (LC-20ADCR, China) and the procedural details were adapted from a previous study ([Lin et al., 2020](#)).

2.5.5 TEM imaging

M. aeruginosa samples, each with a volume of 10 mL, were harvested at specific times (0.25, 0.75, 1.5, 3, 6, and 10 h) through rapid centrifugation at 6000 r/min for 5 min. The resultant sediments were then subsequently treated as reported previously by [Wang et al. \(2011\)](#). TEM was then used to obtain the ultrastructural alteration of *M. aeruginosa* cells treated by $\text{Fe}^0\text{@Mg}(\text{OH})_2$. Meanwhile, crystallographic change of $\text{Fe}^0\text{@Mg}(\text{OH})_2$ were observed using a high-resolution transmission electron microscope (JEM-2100Plus, JEOL, Japan).

2.5.6 Statistical analysis

Figures were created with Origin 2018 (OriginLab, USA) and Prism 8.0 (GraphPad Software, USA). One-way ANOVA was used for determination of the statistical significance ($P < 0.05$) among different test groups.

3 Results

3.1 *M. aeruginosa* removal by $\text{Fe}^0\text{@Mg}(\text{OH})_2$

M. aeruginosa cells rapidly aggregated as flocs within the first 0.75 h by $\text{Fe}^0\text{@Mg}(\text{OH})_2$ treatment (Fig. S1). Hence, the cells in suspensions were efficiently removed via sedimentation. The influence of initial cell densities ($1.0 \times 10^5\text{--}8.0 \times 10^6$ cells/mL) on the removal of *M. aeruginosa* cells by 50 mg/L $\text{Fe}^0\text{@Mg}(\text{OH})_2$ in BG-11 medium was investigated (Fig. 1(a)). Cells were removed rapidly from the water column during 0.5 h in all groups. In general, the removal efficiency of *M. aeruginosa* by $\text{Fe}^0\text{@Mg}(\text{OH})_2$ was enhanced with

increasing initial cell densities. The cell removal efficiency improved from 70% to 97% within 0.5 h treatment, when the initial cell densities increased from 1.0×10^5 to 8.0×10^6 cells/mL. More than 98% of *M. aeruginosa* cells were removed after exposure to $\text{Fe}^0\text{@Mg}(\text{OH})_2$ for 3 h, for the samples with cell densities exceeding 1.0×10^6 cells/mL.

The effect of $\text{Fe}^0\text{@Mg}(\text{OH})_2$ dosages (10–80 mg/L) on the removal efficiency of *M. aeruginosa* cells (cell density = 1.0×10^6 cells/mL) in BG-11 medium was shown in Fig. 1(b). Apparently, the removal efficiency of cyanobacterial cells increased with $\text{Fe}^0\text{@Mg}(\text{OH})_2$ dosages increasing from 10 to 50 mg/L. However, no significant differences ($P > 0.05$) in removal efficiencies were observed at $\text{Fe}^0\text{@Mg}(\text{OH})_2$ dosages > 50 mg/L. For example, 87% and 91% of *M. aeruginosa* cells were removed by 50 and 80 mg/L $\text{Fe}^0\text{@Mg}(\text{OH})_2$ treatment for 1 h, respectively, while the *R* value was only 26% by 10 mg/L $\text{Fe}^0\text{@Mg}(\text{OH})_2$. The removal efficiency of *M. aeruginosa* (1.0×10^6 cells/mL) by

$\text{Fe}^0\text{@Mg}(\text{OH})_2$ treatment in natural water (MHL water) was also assessed, it was lower than that in BG-11 medium initially (Fig. 1(c)). For instance, 20 mg/L $\text{Fe}^0\text{@Mg}(\text{OH})_2$ removed 39% of *M. aeruginosa* cells in BG-11 medium after 0.75 h, while it only removed 19% of cells in MHL water. However, the *R* value of *M. aeruginosa* by $\text{Fe}^0\text{@Mg}(\text{OH})_2$ in MHL water was increased subsequently, and over 98% of cells were removed at a sampling time of 10 h.

3.2 XPS and XRD analysis

The chemical composition and the element change on the surface of *M. aeruginosa* flocs before and after $\text{Fe}^0\text{@Mg}(\text{OH})_2$ treatment were analyzed (Table S2). Fe contents in *M. aeruginosa* flocs increased approximately by 30% and 130%, after dosing with $\text{Fe}^0\text{@Mg}(\text{OH})_2$ for 1.5 and 6 h, respectively. The detailed XPS spectra from 700 to 740 eV presented relative abundances of different Fe species on the

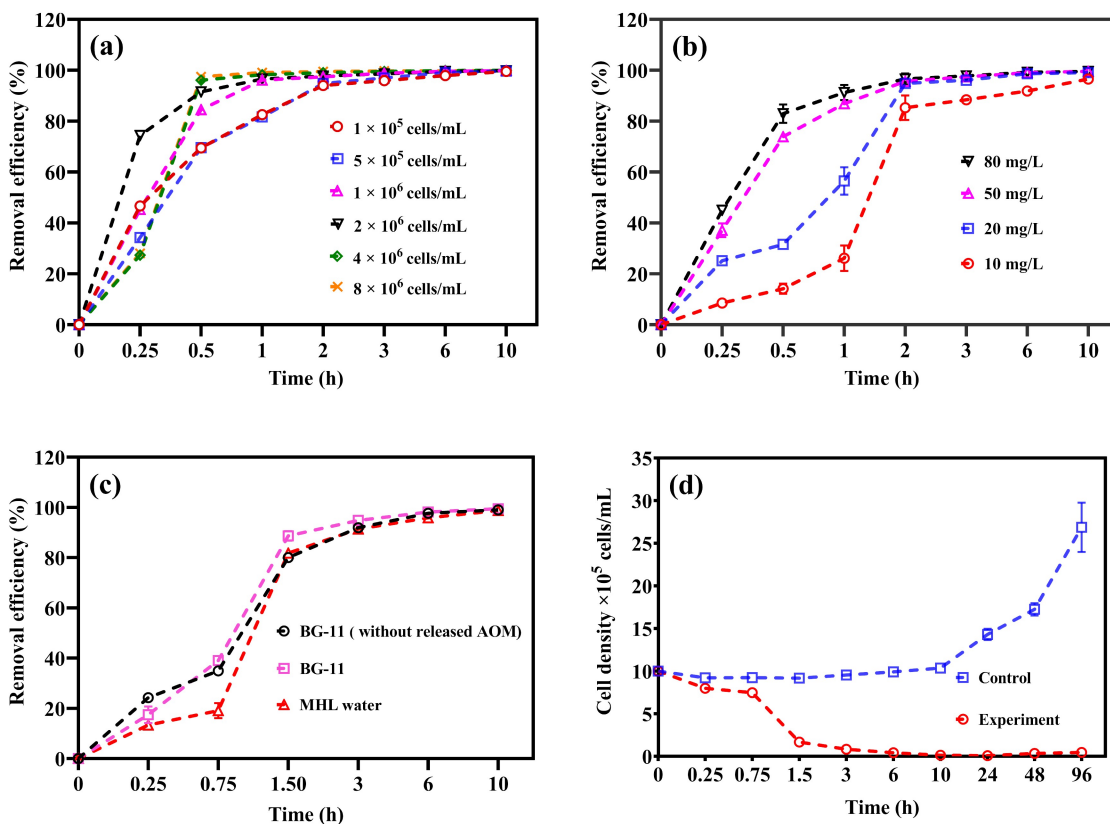


Fig. 1 Removal efficiencies of *M. aeruginosa* by $\text{Fe}^0\text{@Mg}(\text{OH})_2$. (a) the concentration of $\text{Fe}^0\text{@Mg}(\text{OH})_2$ was 50 mg/L, and the water matrix was BG-11 medium; (b) the initial cell density of *M. aeruginosa* was 1.0×10^6 cells/mL, and the water matrix was BG-11 medium; (c) the concentration of $\text{Fe}^0\text{@Mg}(\text{OH})_2$ was 20 mg/L, the initial cell density of *M. aeruginosa* was 1.0×10^6 cells/mL, and the water matrix was BG-11 medium (with and without the released AOM) or MHL water; and (d) the concentration of $\text{Fe}^0\text{@Mg}(\text{OH})_2$ was 20 mg/L, the initial cell density of *M. aeruginosa* was 1.0×10^6 cells/mL, and the water matrix was the MHL water.

surface of *M. aeruginosa* flocs, and the coexistence of Fe(II) and Fe(III) was observed (Fig. 2). The peaks at 710.4 and 724.0 eV correspond to $\text{Fe}^{2+} 2p_{3/2}$ and $\text{Fe}^{2+} 2p_{1/2}$, respectively, and the peaks at 712.4 and 726.1 eV are assigned to $\text{Fe}^{3+} 2p_{3/2}$ and $\text{Fe}^{3+} 2p_{1/2}$ (Zhou et al., 2020). Additionally, the signals of Fe^0 peaks were observed at 706.4 and 719.4 eV, and the peak located at 714.3 eV can be attributed to the Fe(III)-OH (Hu et al., 2018).

Figure 3 presented the XRD plots of the $\text{Fe}^0@\text{Mg}(\text{OH})_2$ particles before and after exposure to SO_4^{2-} solutions. The typical peak at 2θ of 44.68° corresponded to the (110) plane of Fe^0 . Broad peaks at 2θ of 18.58° , 37.98° , and 58.61° were consistent with the (001), (011) and (110) directions of $\text{Mg}(\text{OH})_2$ respectively, which confirmed the formation of $\text{Mg}(\text{OH})_2$ shell. After exposure to SO_4^{2-} solutions, new diffraction peaks appeared at 21.19° and 33.21° , which corresponded to the (110) and (121) directions of FeOOH and Fe_2O_3 , respectively.

3.3 Cell photosynthetic capacity and the variation of K^+

The content of Chl-a in the control sample remained almost constant during the 10 h experiment (Fig. 4(a)). In contrast, with the application of 20 mg/L $\text{Fe}^0@\text{Mg}(\text{OH})_2$, the Chl-a contents in the *M. aeruginosa* suspension gradually decreased to below the detection limit after 1.5 h (Fig. 4(a)). The Fv/Fm value in samples treated with $\text{Fe}^0@\text{Mg}(\text{OH})_2$ maintained at ~ 0.5 during the initial 1.5 h, but dropped to 0.35 after 10 h (Fig. 4(a)). Following the treatment with $\text{Fe}^0@\text{Mg}(\text{OH})_2$ for 0.25 h, the concentration of K^+ in the suspension decreased from 12.6 to 11.8 mg/L ($P < 0.05$) (Fig. 4(b)), and then returned to ~ 12.3 mg/L after 1.5 h.

3.4 Morphology of *M. aeruginosa* cells

The alternations in the ultrastructure of *M. aeruginosa* cells by $\text{Fe}^0@\text{Mg}(\text{OH})_2$ treatment were captured in TEM images (Fig. 5). Intact intracellular structures, including thylakoids, lipid droplets, gas vesicles and nucleoid regions were distinctly observed in the control samples (Fig. 5(b)). Similar ultrastructure of *M. aeruginosa* cells were found after $\text{Fe}^0@\text{Mg}(\text{OH})_2$ treatment for 1.5 h (Fig. 5(c)). Only a small number of cells appeared irregular and rough after 6 and 10 h, yet the majority remained intact (Figs. 5(d)–5(e)). The internalization of $\text{Fe}^0@\text{Mg}(\text{OH})_2$ by *M. aeruginosa* was observed after 10 h of treatment (Fig. 5(f)). Overall, despite being enveloped by $\text{Fe}^0@\text{Mg}(\text{OH})_2$ particles during the treatment, incidents of cell collapse and lysis were rarely observed in *M. aeruginosa* samples (Figs. 5(c)–5(f)).

3.5 Variations of MC-LR and AOM in *M. aeruginosa* samples

The *M. aeruginosa* samples treated with 20 mg/L $\text{Fe}^0@\text{Mg}(\text{OH})_2$ for 0–10 h were collected and measured for MCs (Fig. 4(b)). The concentration of extracellular MC-LR in the control samples remained at around 1.8 $\mu\text{g/L}$. Following the treatment with $\text{Fe}^0@\text{Mg}(\text{OH})_2$ for 0.25 h, the concentration of MC-LR decreased from 1.8 to 1.4 $\mu\text{g/L}$, and then remained relatively stable thereafter. Additionally, the main components of dissolved AOM in the *M. aeruginosa* cells were also assessed using EEM fluorescence spectra (Fig. 6). Only one main peak at Ex/Em of 275/320 nm was identified at each sampling time, indicating the presence of soluble microbial products as described by Chen et al. (2003).

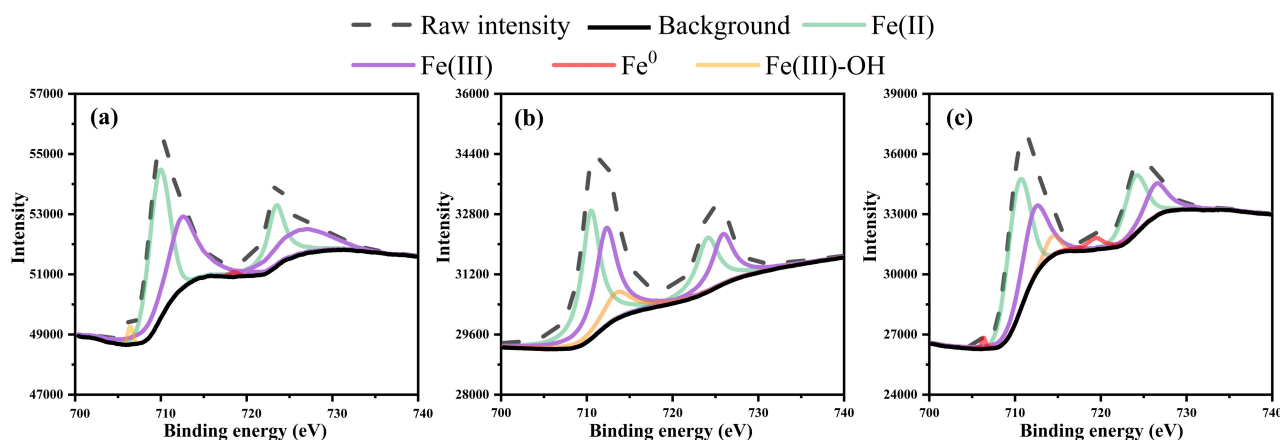


Fig. 2 XPS spectra analysis. (a) $\text{Fe}^0@\text{Mg}(\text{OH})_2$, (b) and (c) flocs of *M. aeruginosa* after the $\text{Fe}^0@\text{Mg}(\text{OH})_2$ exposure for 1.5 and 6 h.

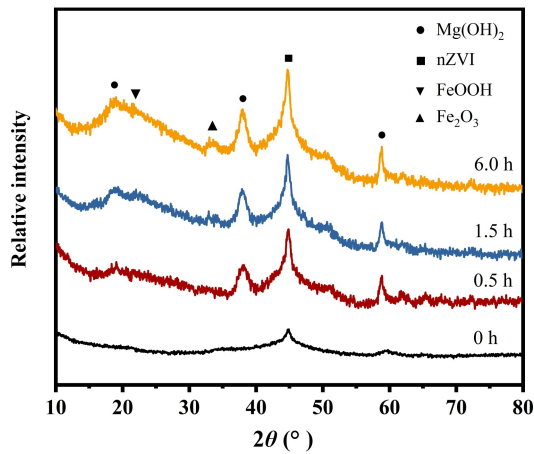


Fig. 3 XRD patterns of Fe⁰@Mg(OH)₂ before and after reaction with SO₄²⁻ (Fe:SO₄²⁻ = 1:3, wt%) for 0, 0.5, 1.5, and 6 h.

4 Discussion

4.1 Factors affecting the removal efficiency of *M. aeruginosa* by Fe⁰@Mg(OH)₂ and related mechanisms

M. aeruginosa with cell densities varying from 1.0 × 10⁵ cells/mL to 8.0 × 10⁶ cells/mL, could be effectively removed from suspensions by Fe⁰@Mg(OH)₂ (Figs. 1(a) and S1). Besides simplifying the operation, Fe⁰@Mg(OH)₂ can achieve higher efficiency in *M. aeruginosa* removal, in comparison with traditional methods that combine pre-oxidation, coagulation, and sedimentation (Takaara et al., 2010; Qi et al., 2016). A previous study also indicated that Fe⁰@Mg(OH)₂ could lead to efficient *M. aeruginosa* removal at a cell density of 2.5 × 10⁶ cells/mL, in which magnetic attraction between Fe⁰@Mg(OH)₂ particles and cells was identified as the main removal mechanism (Fan et al., 2018a). In the current study, Fe(III) ions were gradually generated during the Fe⁰@Mg(OH)₂ treatment (Fig. 2).

These *in situ* formed Fe(III) ions could act as potential cation bridges between *M. aeruginosa* cells and Fe⁰@Mg(OH)₂ particles, hence facilitating the aggregation of cells and increasing the size of cyanobacterial flocs (Ma et al., 2012). Notably, the *R* values of *M. aeruginosa* by Fe⁰@Mg(OH)₂ was found to increase with increasing cell densities, but decreased upon the removal of dissolved AOM (Figs. 1(a)–1(c)). Both the surface charge of *M. aeruginosa* cells and AOM are negative, in contrast to the positive charge of Fe⁰@Mg(OH)₂ (Henderson et al., 2008; Ma et al., 2012; Qu et al., 2012). Therefore, the formation and sedimentation of complexes comprising cells, Fe⁰@Mg(OH)₂, and AOM could be enhanced by increasing the amounts of cells and associated AOM.

The pseudo-second-order equation was used to describe *M. aeruginosa* removal after exposure to Fe⁰@Mg(OH)₂, which is shown in the following Eq. (2) (Hamadi et al., 2004).

$$\frac{t}{q_t} = \frac{1}{kq_e^2} + \frac{t}{q_e} \quad (2)$$

where *q_t* represents the amount of *M. aeruginosa* cells removed by Fe⁰@Mg(OH)₂ at time *t* (cells/μg), *q_e* represents the amount of *M. aeruginosa* cell removal at equilibrium (cells/μg), *k* represents the rate constant for cell removal (μg/(cells·h)) and *kq_e²* is the initial cell removal rate constant (cells/(μg·h)).

The removal rate constant (*k*) remained almost consistent throughout the treatment period. This may be owing to the substantial removal of *M. aeruginosa* cells within the first hour by 50 mg/L Fe⁰@Mg(OH)₂. Therefore, the initial removal rates were calculated to evaluate the cell removal ability (Table 1). The rate of cell removal was dependent on initial cell density, increasing from 10 to 16667 cells/(μg·h) as the initial cell densities increased. However, the initial removal

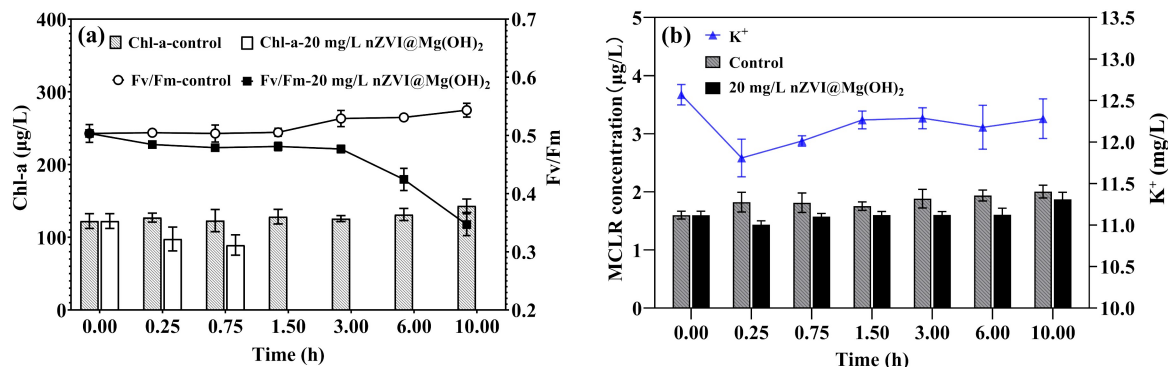


Fig. 4 Variations of (a) Chl-a and Fv/Fm, (b) extracellular MC-LR and K⁺ in the *M. aeruginosa* suspension (the initial cell density was 1.0 × 10⁶ cells/mL) dosed with 20 mg/L Fe⁰@Mg(OH)₂.

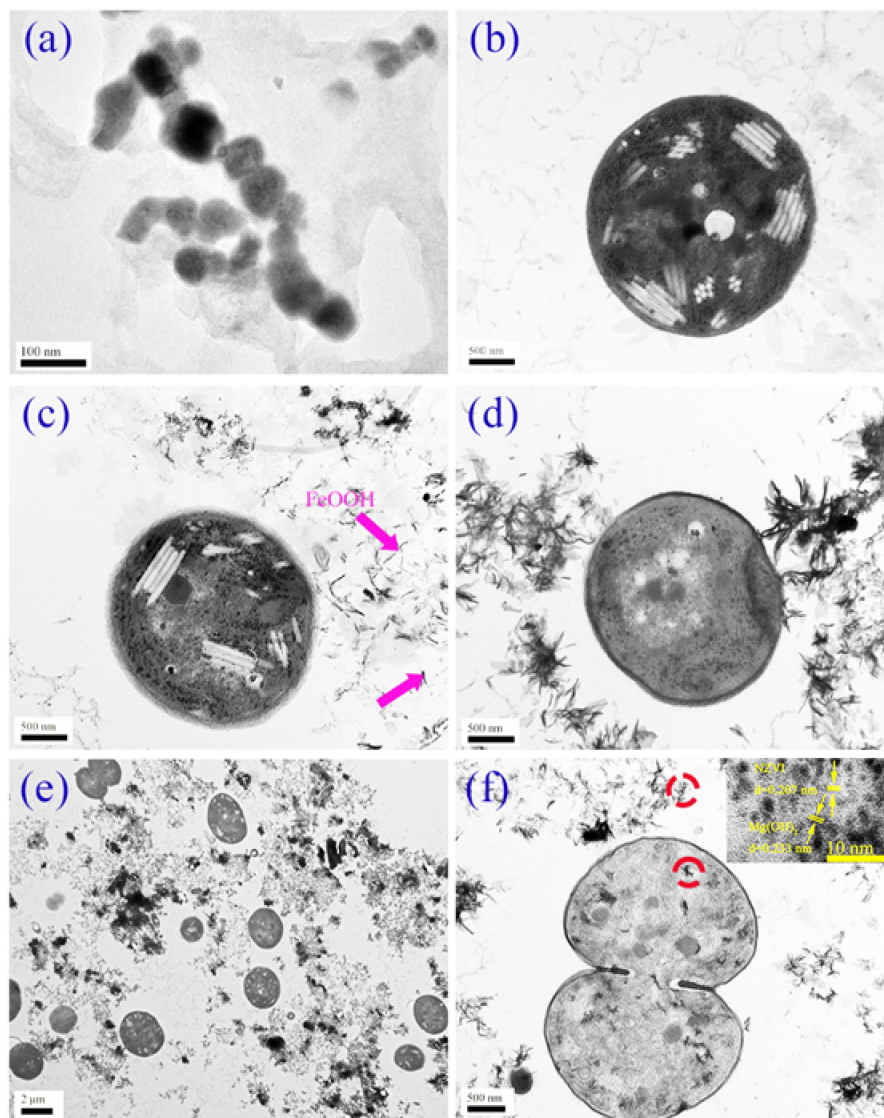


Fig. 5 TEM images of (a) $\text{Fe}^0\text{@Mg(OH)}_2$ ultrathin slices of *M. aeruginosa* (1.0×10^6 cells/mL) after exposure to $\text{Fe}^0\text{@Mg(OH)}_2$ (20 mg/L) for (b) 0, (c) 1.5, (d) 6, (e) and (f) 10 h. Pink arrows in (c) represent the presence of FeOOH , and the HRTEM image was selected from the red-circled region in (f).

rate of *M. aeruginosa* increased slightly with increasing $\text{Fe}^0\text{@Mg(OH)}_2$ dosages (Table 2). It only increased from 47 to 135 cells/ $(\mu\text{g}\cdot\text{h})$ when the $\text{Fe}^0\text{@Mg(OH)}_2$ dosages increased from 10 to 80 mg/L (Table 2). Overall, $\text{Fe}^0\text{@Mg(OH)}_2$ demonstrated outstanding performance in the treatment of high concentrations of cyanobacteria, while some other nanocomposites (e.g., Fe-Cu-Mn oxides/peroxymonosulfate) are limited to treating cyanobacterial samples with low cell densities (Sun et al., 2022; Yang et al., 2023).

The efficient removal of *M. aeruginosa* by $\text{Fe}^0\text{@Mg(OH)}_2$ in natural waters has also been confirmed in this study (Figs. 1(c) and 4(a)). Initially, within the first 1.5 h, there was a decrease in the

removal efficiency of *M. aeruginosa* (Fig. 1(c)). The presence of a high concentration of SO_4^{2-} in MHL water (68.5 mg/L) may have accelerated the passivation of the core-shell structure of $\text{Fe}^0\text{@Mg(OH)}_2$ (Xie and Cwiertny, 2012; Pullin et al., 2017), which was verified by the observation of FeOOH transformed from $\text{Fe}^0\text{@Mg(OH)}_2$ (Figs. 3 and 5) (Zhou et al., 2014). A study by Teixeira and Rosa (2007) has reported that the efficiency of Al_2O_3 in *M. aeruginosa* removal was decreased in natural water, requiring higher Al_2O_3 dosages. However, the removal efficiency of *M. aeruginosa* by $\text{Fe}^0\text{@Mg(OH)}_2$ could subsequently exceed 98% in MHL water after 1.5 h without increase in dosages (Fig. 1(b)). Besides, no cyanobacterial

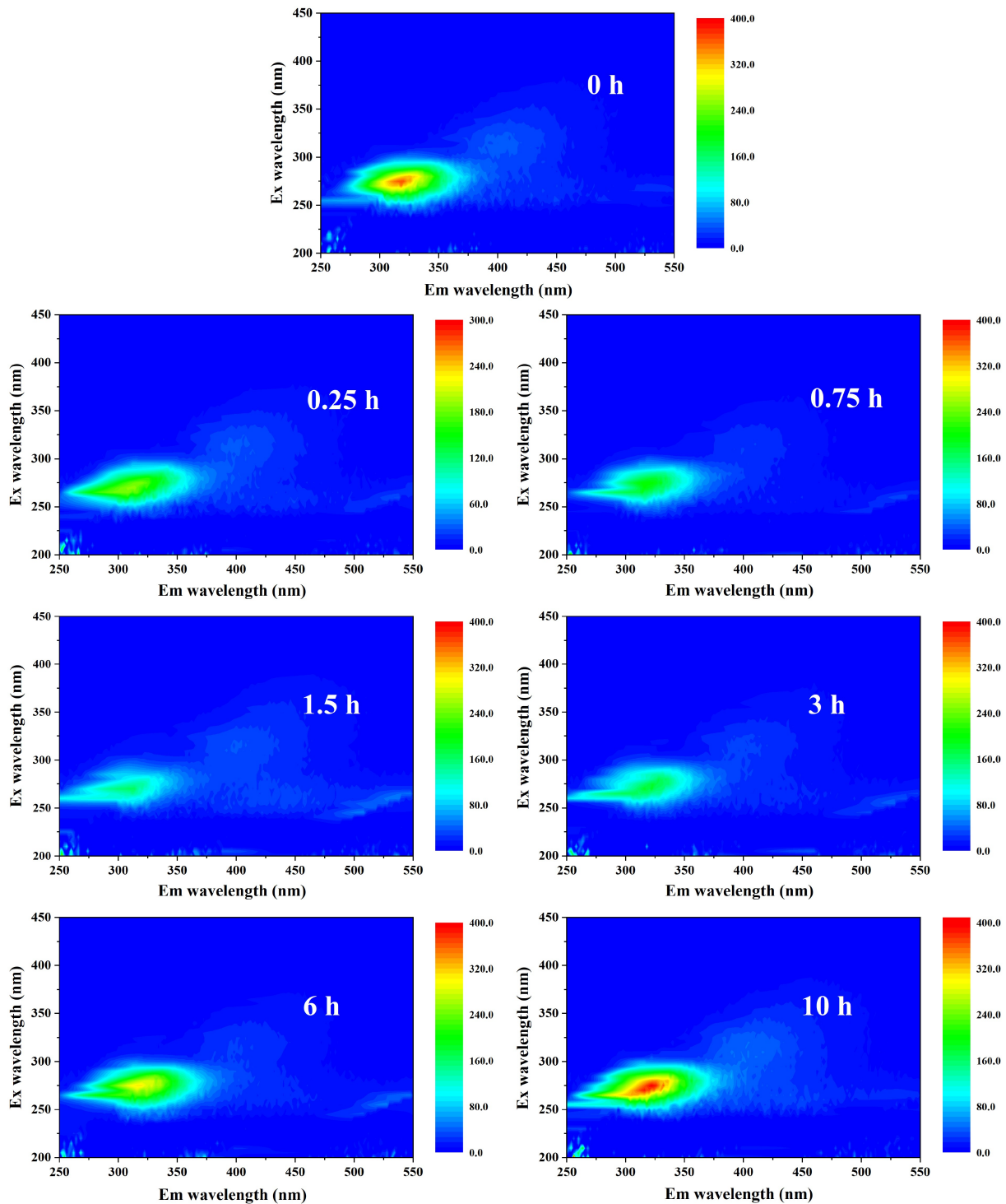


Fig. 6 EEM fluorescence spectra of the released AOM in the *M. aeruginosa* samples after $\text{Fe}^0@Mg(OH)_2$ treatment for 0, 0.25, 0.75, 1.5, 3, 6, and 10 h, with a dosage of 20 mg/L.

regrowth was observed (Fig. 1(d)). Therefore, $\text{Fe}^0@Mg(OH)_2$ demonstrates a high potential to efficiently mitigate cyanobacteria problems, even in complex aquatic environments.

4.2 The characteristics of *M. aeruginosa* samples after exposure to $\text{Fe}^0@Mg(OH)_2$

As a critical component to biosynthesize cytoplasmic

Table 1 The pseudo-second-order kinetics for *M. aeruginosa* removal by Fe⁰@Mg(OH)₂, with different initial cell densities

| Initial cell densities (cells/mL) | q_e (10 ⁵ cells/μg) | k (μg/(cells·h)) | Initial removal rate (cells/(μg·h)) |
|-----------------------------------|----------------------------------|--------------------|-------------------------------------|
| 1 × 10 ⁵ | 2.03 | 2.40 | 10 |
| 5 × 10 ⁵ | 10.19 | 0.50 | 52 |
| 1 × 10 ⁶ | 20.12 | 0.75 | 303 |
| 2 × 10 ⁶ | 40.16 | 0.52 | 833 |
| 4 × 10 ⁶ | 80.00 | 0.52 | 3333 |
| 8 × 10 ⁶ | 158.73 | 0.66 | 16667 |

Table 2 The pseudo-second-order kinetics for *M. aeruginosa* removal by Fe⁰@Mg(OH)₂ with different dosages

| Fe ⁰ @Mg(OH) ₂ dosages (mg/L) | q_e (10 ⁵ cells/μg) | k (μg/(cells·h)) | Initial removal rate (cells/(μg·h)) |
|---|----------------------------------|--------------------|-------------------------------------|
| 10 | 129.87 | 0.003 | 47 |
| 20 | 54.35 | 0.025 | 75 |
| 50 | 20.24 | 0.334 | 137 |
| 80 | 12.56 | 0.856 | 135 |

membranes, the concentration of dissolved K⁺ is usually used to assess the cell integrity of *M. aeruginosa* (Zhou et al., 2013; 2020). In this study, a decrease of K⁺ was observed during the first 0.25 h, likely due to the adsorption by Fe⁰@Mg(OH)₂ (Fig. 4(b)). A similar phenomenon was reported by Li and Zhang (2007), indicating that metal cations could be adsorbed onto the surface of Fe⁰. Although the adsorbed K⁺ was subsequently desorbed, its concentration remained below the initial level during the 10-h treatment (Fig. 4(b)). The steady trend of K⁺ during the treatment suggested that the *M. aeruginosa* cells probably remained intact. In addition, humic-like substances, decomposition products of dead cells, were not observed in the *M. aeruginosa* samples throughout the treatment (Fig. 6), indicating that Fe⁰@Mg(OH)₂ did not induce additional damage to the cells (Qu et al., 2012; Xu et al., 2016).

Fv/Fm value, being biomass-independent, serves as a sensitive indicator for assessing the PSII function in photosynthetic organisms (Maxwell and Johnson, 2000; Drábková et al., 2007). The Fv/Fm values of *M. aeruginosa* samples diminished after 1.5 h treatment with 20 mg/L Fe⁰@Mg(OH)₂ (Fig. 4), and the particles were found to attach on *M. aeruginosa* cells (Fig. 5). These findings suggest that the adhesion of Fe⁰@Mg(OH)₂ on the cell surface may limit the accessibility of *M. aeruginosa* to light, echoing the effects observed from other nanoparticles, thus hindering cell regrowth (Fig. 1(d)) (Wang et al., 2011; Long et al., 2014). Furthermore, similarly to the impact

of other nanoparticles, the internalization of Fe⁰@Mg(OH)₂ by *M. aeruginosa* cells may also impede their photosynthesis (Fig. 5(f)) (Wang et al., 2011).

In general, the levels of extracellular MC-LR in the *M. aeruginosa* samples treated with Fe⁰@Mg(OH)₂ were comparable to those in the control, with a notable decrease observed within the first 0.25 h (Fig. 4(b)). Given the minimal oxidation capacity of Fe⁰@Mg(OH)₂, this reduction in MC-LR levels could be attributed to the adsorption capacity of FeOOH (Pivokonsky et al., 2012), which was formed from Fe⁰@Mg(OH)₂ process (Fig. 3). This indicates that Fe⁰@Mg(OH)₂ presents an effective method to mitigate cyanobacterial problems without increase in dissolved toxins, which is a significant advantage over other technologies (Teixeira and Rosa, 2006; Wang et al., 2018). For instance, it has been reported that static ultrasonic radiation would induce damage to *M. aeruginosa* cells, resulting in increased concentrations of released MC-LR as ultrasonic radiation time increased (Peng et al., 2023). Similarly, chemical options such as oxidants have the potential to lyse cyanobacterial cells, and improper oxidant dosage would also induce the release of MC-LR, deteriorating water quality (Ou et al., 2012; Zhang et al., 2017).

5 Conclusions

This study demonstrates that Fe⁰@Mg(OH)₂ can effectively remove *M. aeruginosa* with high cell densities in natural water. The negligible release of MCs and AOM during the Fe⁰@Mg(OH)₂ treatment can avoid worsening water quality and reduce the burden on subsequent treatment processes. The effectiveness of Fe⁰@Mg(OH)₂ may be influenced by the water matrix at the start of treatment, while it could be enhanced subsequently without increasing its dosage. Given its high efficiency, Fe⁰@Mg(OH)₂ has the potential for broad applications in immediate control of *M. aeruginosa* blooms across various water bodies, including ponds, reservoirs, lakes and landscape waters.

Conflict of Interests The authors declare that the research was conducted in the absence of any commercial or financial relationships that could be construed as a potential conflict of interest.

Acknowledgements This study was supported by the National Natural Science Foundation of China (Nos. 51708490 and 41730316). We would like to thank Prof. Tsair-Fuh Lin for his valuable advice.

Electronic Supplementary Material Supplementary material is

available in the online version of this article at <https://doi.org/10.1007/s11783-025-1975-x> and is accessible for authorized users.

References

- Chen C, Zhang X, Jiang T, Li M, Peng Y, Liu X, Ye J, Hua Y (2021). Removal of uranium(VI) from aqueous solution by Mg(OH)₂-coated nanoscale zero-valent iron: reactivity and mechanism. *Journal of Environmental Chemical Engineering*, 9(1): 104706
- Chen W, Westerhoff P, Leenheer J A, Booksh K (2003). Fluorescence excitation-emission matrix regional integration to quantify spectra for dissolved organic matter. *Environmental Science & Technology*, 37(24): 5701–5710
- Codd G A, Morrison L F, Metcalf J S (2005). Cyanobacterial toxins: risk management for health protection. *Toxicology and Applied Pharmacology*, 203(3): 264–272
- Drábková M, Admiraal W, Marsálek B (2007). Combined exposure to hydrogen peroxide and light-selective effects on cyanobacteria, green algae, and diatoms. *Environmental Science & Technology*, 41(1): 309–314
- Eljamal O, Mokete R, Matsunaga N, Sugihara Y (2018). Chemical pathways of nanoscale zero-valent iron (NZVI) during its transformation in aqueous solutions. *Journal of Environmental Chemical Engineering*, 6(5): 6207–6220
- Fan J, Daly R, Hobson P, Ho L, Brookes J (2013). Impact of potassium permanganate on cyanobacterial cell integrity and toxin release and degradation. *Chemosphere*, 92(5): 529–534
- Fan J, Hu Y B, Li X Y (2018a). Nanoscale zero-valent iron coated with magnesium hydroxide for effective removal of cyanobacteria from water. *ACS Sustainable Chemistry & Engineering*, 6(11): 15135–15142
- Fan J, Lin B H, Chang C W, Zhang Y, Lin T F (2018b). Evaluation of potassium ferrate as an alternative disinfectant on cyanobacteria inactivation and associated toxin fate in various waters. *Water Research*, 129: 199–207
- Fang J, Ma J, Yang X, Shang C (2010). Formation of carbonaceous and nitrogenous disinfection by-products from the chlorination of *Microcystis aeruginosa*. *Water Research*, 44(6): 1934–1940
- Gao Q T, Tam N F Y (2011). Growth, photosynthesis and antioxidant responses of two microalgal species, *Chlorella vulgaris* and *Selenastrum capricornutum*, to nonylphenol stress. *Chemosphere*, 82(3): 346–354
- Ger K A, Hansson L A, Lurling M (2014). Understanding cyanobacteria-zooplankton interactions in a more eutrophic world. *Freshwater Biology*, 59(9): 1783–1798
- Gobler C J (2020). Climate change and harmful algal blooms: insights and perspective. *Harmful Algae*, 91: 101731
- Hamadi N K, Swaminathan S, Chen X D (2004). Adsorption of Paraquat dichloride from aqueous solution by activated carbon derived from used tires. *Journal of Hazardous Materials*, 112(1–2): 133–141
- Henderson R K, Baker A, Parsons S A, Jefferson B (2008). Characterisation of algogenic organic matter extracted from cyanobacteria, green algae and diatoms. *Water Research*, 42(13): 3435–3445
- Hu Y, Zhang M, Qiu R, Li X (2018). Encapsulating nanoscale zero-valent iron with a soluble Mg(OH)₂ shell for improved mobility and controlled reactivity release. *Journal of Materials Chemistry. A, Materials for Energy and Sustainability*, 6(6): 2517–2526
- Hu Y B, Zhang M, Li X Y (2019). Improved longevity of nanoscale zero-valent iron with a magnesium hydroxide coating shell for the removal of Cr(VI) in sand columns. *Environment International*, 133: 105249
- Huo X, Chang D W, Tseng J H, Burch M D, Lin T F (2015). Exposure of *Microcystis aeruginosa* to hydrogen peroxide under light: kinetic modeling of cell rupture and simultaneous microcystin degradation. *Environmental Science & Technology*, 49(9): 5502–5510
- Jia P, Zhou Y, Zhang X, Zhang Y, Dai R (2018). Cyanobacterium removal and control of algal organic matter (AOM) release by UV/H₂O₂ pre-oxidation enhanced Fe(II) coagulation. *Water Research*, 131: 122–130
- Jian Z, Bai Y, Chang Y, Liang J, Qu J (2019). Removal of micropollutants and cyanobacteria from drinking water using KMnO₄ pre-oxidation coupled with bioaugmentation. *Chemosphere*, 215: 1–7
- Lei C, Zhang L, Yang K, Zhu L, Lin D (2016). Toxicity of iron-based nanoparticles to green algae: effects of particle size, crystal phase, oxidation state and environmental aging. *Environmental Pollution*, 218: 505–512
- Li L, Wang Z, Rietveld L C, Gao N, Hu J, Yin D, Yu S (2014). Comparison of the effects of extracellular and intracellular organic matter extracted from *Microcystis aeruginosa* on ultrafiltration membrane fouling: dynamics and mechanisms. *Environmental Science & Technology*, 48(24): 14549–14557
- Li X Q, Zhang W X (2007). Sequestration of metal cations with zerovalent iron nanoparticles-A study with high resolution X-ray photoelectron spectroscopy (HR-XPS). *Journal of Physical Chemistry C*, 111(19): 6939–6946
- Lin S, Yu X, Fang J, Fan J (2020). Influences of the micropollutant erythromycin on cyanobacteria treatment with potassium permanganate. *Water Research*, 177: 115786
- Lin T F, Chang D W, Lien S K, Tseng Y S, Chiu Y T, Wang Y S (2009). Effect of chlorination on the cell integrity of two noxious cyanobacteria and their releases of odorants. *Journal Of Water Supply Research and Technology-Aqua*, 58: 539–551.
- Long Z, Ji J, Yang K, Lin D, Wu F (2014). Systematic and quantitative investigation of the mechanism of carbon nanotubes' toxicity toward algae. *Environmental Science & Technology*, 48(8): 4634
- Ma J, Lei G, Fang J (2007). Effect of algae species population structure on their removal by coagulation and filtration processes: a case study. *Journal of Water Supply: Research & Technology-Aqua*, 56(1): 41–54

- Ma M, Liu R, Liu H, Qu J (2012). Effect of moderate pre-oxidation on the removal of *Microcystis aeruginosa* by KMnO_4 -Fe(II) process: significance of the *in-situ* formed Fe(III). *Water Research*, 46(1): 73–81
- Ma X, Wang Y, Feng S, Wang S (2015). Vertical migration patterns of different phytoplankton species during a summer bloom in Dianchi Lake, China. *Environmental Earth Sciences*, 74(5): 3805–3814
- Marsalek B, Jancula D, Marsalkova E, Mashlan M, Safarova K, Tucek J, Zboril R (2012). Multimodal action and selective toxicity of zerovalent iron nanoparticles against cyanobacteria. *Environmental Science & Technology*, 46(4): 2316–2323
- Maxwell K, Johnson G N (2000). Chlorophyll fluorescence: a practical guide. *Journal of Experimental Botany*, 51(345): 659–668
- Naceradska J, Pivokonsky M, Pivokonska L, Baresova M, Henderson R K, Zamyadi A, Janda V (2017). The impact of pre-oxidation with potassium permanganate on cyanobacterial organic matter removal by coagulation. *Water Research*, 114: 42–49
- Nguyen N H A, Spanek R, Kasalicky V, Ribas D, Vlkova D, Rehakova H, Kejzlar P, Sevcu A (2018). Different effects of nano-scale and micro-scale zero-valent iron particles on planktonic microorganisms from natural reservoir water. *Environmental Science. Nano*, 5(5): 1117–1129
- Nicholson B C, Rositano J, Burch M D (1994). Destruction of cyanobacterial peptide hepatotoxins by chlorine and chloramine. *Water Research*, 28(6): 1297–1303
- Ou H, Gao N, Deng Y, Qiao J, Wang H (2012). Immediate and long-term impacts of UV-C irradiation on photosynthetic capacity, survival and microcystin-LR release risk of *Microcystis aeruginosa*. *Water Research*, 46: 1241–1250
- Paerl H W, Scott J T (2010). Throwing fuel on the fire: synergistic effects of excessive nitrogen inputs and global warming on harmful algal blooms. *Environmental Science & Technology*, 44(20): 7756–7758
- Peng Y, Yang X, Ren B, Zhang Z, Deng X, Yin W, Zhou S, Yang S (2023). Algae removal characteristics of the ultrasonic radiation enhanced drinking water treatment process. *Journal of Water Process Engineering*, 55: 104154
- Pivokonsky M, Safarikova J, Bubakova P, Pivokonska L (2012). Coagulation of peptides and proteins produced by *Microcystis aeruginosa*: interaction mechanisms and the effect of Fe-peptide/protein complexes formation. *Water Research*, 46(17): 5583–5590
- Pullin H, Crane R A, Morgan D J, Scott T B (2017). The effect of common groundwater anions on the aqueous corrosion of zero-valent iron nanoparticles and associated removal of aqueous copper and zinc. *Journal of Environmental Chemical Engineering*, 5(1): 1166–1173
- Qi J, Lan H, Miao S, Xu Q, Liu R, Liu H, Qu J (2016). KMnO_4 -Fe(II) pretreatment to enhance *Microcystis aeruginosa* removal by aluminum coagulation: does it work after long distance transportation? *Water Research*, 88: 127–134
- Qu F, Liang H, He J, Ma J, Wang Z, Yu H, Li G (2012). Characterization of dissolved extracellular organic matter (dEOM) and bound extracellular organic matter (bEOM) of *Microcystis aeruginosa* and their impacts on UF membrane fouling. *Water Research*, 46(9): 2881–2890
- Rajasekhar P, Fan L, Nguyen T, Roddick F A (2012). A review of the use of sonication to control cyanobacterial blooms. *Water Research*, 46(14): 4319–4329
- Stanier R Y, Kunisawa R, Mandel M, Cohen-Bazire G (1971). Purification and properties of unicellular blue-green algae (order *Chroococcales*). *Bacteriological Reviews*, 35: 171–205
- Sun S, Tang Q, Yu T, Gao Y, Zhang W, Zhou L, Elhegazy H, He K (2022). Fabrication of $\text{g-C}_3\text{N}_4/\text{Bi}_2\text{MoO}_6/\text{AgI}$ floating sponge for photocatalytic inactivation of *Microcystis aeruginosa* under visible light br. *Environmental Research*, 215: 114216
- Tang Y, Xin H, Yang S, Guo M, Malkoske T, Yin D, Xia S (2018). Environmental risks of ZnO nanoparticle exposure on *Microcystis aeruginosa*: toxic effects and environmental feedback. *Aquatic Toxicology*, 204(13): 19–26
- Teixeira M R, Rosa M J (2006). Integration of dissolved gas flotation and nanofiltration for *M. aeruginosa* and associated microcystins removal. *Water Research*, 40(19): 3612–3620
- Teixeira M R, Rosa M J (2007). Comparing dissolved air flotation and conventional sedimentation to remove cyanobacterial cells of *Microcystis aeruginosa*. Part II. The effect of water background organics. *Separation and Purification Technology*, 53(1): 126–134
- Wang J, Chen Z, Chen H, Wen Y (2018). Effect of hydrogen peroxide on *Microcystis aeruginosa*: role of cytochromes P450. *Science of the Total Environment*, 626: 211–218
- Wang Z, Li J, Zhao J, Xing B (2011). Toxicity and internalization of CuO nanoparticles to prokaryotic alga *Microcystis aeruginosa* as affected by dissolved organic matter. *Environmental Science & Technology*, 45(14): 6032–6040
- Wu Z X, Gan N Q, Huang Q, Song L R (2007). Response of *Microcystis* to copper stress—Do phenotypes of *Microcystis* make a difference in stress tolerance? *Environmental Pollution*, 147(2): 324–330
- Xie P, Ma J, Fang J, Guan Y, Yue S, Li X, Chen L (2013). Comparison of permanganate preoxidation and preozonation on algae containing water: cell integrity, characteristics, and chlorinated disinfection byproduct formation. *Environmental Science & Technology*, 47(24): 14051–14061
- Xie Y, Cwiertny D M (2012). Influence of anionic cosolutes and pH on nanoscale zerovalent iron longevity: time scales and mechanisms of reactivity loss toward 1,1,1,2-tetrachloroethane and Cr(VI). *Environmental Science & Technology*, 46(15): 8365–8373
- Xu H, Pei H, Xiao H, Li X, Ma C, Hu W (2016). Inactivation of *Microcystis aeruginosa* by hydrogen-terminated porous Si wafer: performance and mechanisms. *Journal of Photochemistry and Photobiology. B, Biology*, 158: 23–29

- Yang Z, Hou J, Wu J, Miao L (2023). Mesoporous carbon framework supported Fe-Cu-Mn oxides as an efficient peroxymonosulfate catalyst for the control of harmful algal blooms: synergism of Fe-Cu-Mn and role of mesoporous carbon. *Chemical Engineering Journal*, 461: 141877
- Zamyadi A, Macleod S L, Fan Y, Mcquaid N, Dorner S, Sauve S, Prevost M (2012). Toxic cyanobacterial breakthrough and accumulation in a drinking water plant: a monitoring and treatment challenge. *Water Research*, 46(5): 1511–1523
- Zhang B, Jiang D, Guo X, He Y, Ong C N, Xu Y, Pal A (2015). Removal of *Microcystis aeruginosa* using nano-Fe₃O₄ particles as a coagulant aid. *Environmental Science and Pollution Research International*, 22(23): 18731–18740
- Zhang H, Dan Y, Adams C D, Shi H, Ma Y, Eichholz T (2017). Effect of oxidant demand on the release and degradation of microcystin-LR from *Microcystis aeruginosa* during oxidation. *Chemosphere*, 181: 562–568
- Zhang K, Lin T F, Zhang T, Li C, Gao N (2013). Characterization of typical taste and odor compounds formed by *Microcystis aeruginosa*. *Journal of Environmental Sciences*, 25(8): 1539–1548
- Zhang X, Devanadera M C E, Roddick F A, Fan L, Dalida M L P (2016). Impact of algal organic matter released from *Microcystis aeruginosa* and *Chlorella* sp. on the fouling of a ceramic microfiltration membrane. *Water Research*, 103: 391–400
- Zhou J, Liu J, Zhao Z, Peng W, Cui F, Liang Z (2020). *Microcystis aeruginosa*-laden water treatment using peroxymonosulfate enhanced Fe(II) coagulation: performance and the role of *in situ* formed Fe₃O₄. *Chemical Engineering Journal*, 382: 123012
- Zhou L, Thanh T L, Gong J, Kim J H, Kim E J, Chang Y S (2014). Carboxymethyl cellulose coating decreases toxicity and oxidizing capacity of nanoscale zerovalent iron. *Chemosphere*, 104: 155–161
- Zhou S, Shao Y, Gao N, Deng Y, Qiao J, Ou H, Deng J (2013). Effects of different algaecides on the photosynthetic capacity, cell integrity and microcystin-LR release of *Microcystis aeruginosa*. *Science of the Total Environment*, 463-464: 111–119